Artesunate alleviates interleukin-1β-induced inflammatory response and apoptosis by inhibiting the NF-κB signaling pathway in chondrocyte-like ATDC5 cells, and delays the progression of osteoarthritis in a mouse model

YICHENG LI[1*], WENBO MU[1*], JIANGDONG REN[1], SHALITANATI WUERMANBIEKE[1], TUERHONGJIANG WAHAFU[1], BAOCHAO JI[1], HAIRONG MA[2], ABDUSAMI AMAT[1], KEYUAN ZHANG[1] and LI CAO[1]

[1]Department of Orthopedics, First Affiliated Hospital of Xinjiang Medical University; [2]State Key Laboratory of Pathogenesis, Prevention and Treatment of High Incidence Diseases in Central Asian Xinjiang Key Laboratory of Echinococcosis, Clinical Medical Research Institute, First Affiliated Hospital of Xinjiang Medical University, Urumqi, Xinjiang 830054, P.R. China

Received January 23, 2019; Accepted May 7, 2019

DOI: 10.3892/ijmm.2019.4290

Abstract. Osteoarthritis (OA) is a progressive and degenerative joint disorder that is highly prevalent worldwide and for which there is currently no effective medical therapy. Artesunate (ART), a natural compound used to treat malaria, possesses diverse biological properties, including the regulation of inflammation and apoptosis in various cells; however, its role in OA remains unclear. The aim of the present study was to investigate the effects of ART on interleukin (IL)-1β-induced chondrocyte-like ATDC5 cells and in an OA mouse model. The results revealed that ART dose-dependently relieved the inhibitory effect of IL-1β on cell viability. Moreover, ART significantly reduced the overexpression of matrix metalloproteinase (MMP)-3, MMP-13, a disintegrin and metalloproteinase with thrombospondin motifs-5 and cyclooxygenase-2 at both the gene and protein levels in chondrocyte-like ATDC5 cells stimulated by IL-1β. Furthermore, ART decreased the expression of pro-apoptotic Bax, cleaved caspase-3 and cleaved caspase-7 in a dose-dependent manner, and increased the expression of the anti-apoptotic factor Bcl-2. These changes were mediated by the inhibitory effect of ART on the nuclear factor-κB signaling pathway, defined as repression of the phosphorylation of IκBα and p65, and improved redistribution of p65. Additionally, ART blocked the advancement of the calcified cartilage zone and the loss of proteoglycan, and lowered histological scoring of OA in a mouse model. Taken together, these results indicate that ART may be of value as a therapeutic agent for OA.

Correspondence to: Professor Li Cao, Department of Orthopedics, First Affiliated Hospital of Xinjiang Medical University, 137 South Liyushan Road, Urumqi, Xinjiang 830054, P.R. China
Email: xjbone@sina.com

*Contributed equally

Key words: artesunate, inflammatory response, apoptosis, chondrocytes, osteoarthritis

Introduction

Osteoarthritis (OA) is the most common degenerative joint disease, afflicting mainly the weight-bearing joints. It is estimated that >50 million individuals in the USA will be affected by the year 2020 (1). The clinical symptoms of OA include chronic joint pain, limited movement and irreversible joint dysfunction, all of which are caused by synovitis, articular cartilage degeneration, osteophyte formation and subchondral bone sclerosis (2). Data from the Global Burden of Disease study in 2010 revealed that OA of the hip and knee was ranked as the 11th highest contributor to global disability and the 38th highest contributor to disability-adjusted life years (3). Despite the identification of risk factors, such as ageing, obesity and metabolic disorders, no effective interventions for preventing the progression of OA are currently available. Therefore, there is an urgent need for more effective and safe therapies for OA.

Chondrocytes, the unique cells in the articular cartilage, are responsible for synthesizing and regenerating extracellular matrix (ECM), which is primarily composed of type II collagen and proteoglycan (4). During the course of OA, the overproduction of pro-inflammatory cytokines, such as interleukin (IL)-1β and tumor necrosis factor (TNF)-α, induces chondrocytes to secrete proteolytic enzymes, such as matrix metalloproteinases (MMPs) and a disintegrin and metalloproteinase with thrombospondin motifs (ADAMTs), resulting in the loss of the major components of the ECM (5,6) and even the occurrence of apoptosis (7). Additionally, IL-1β has been confirmed to stimulate the activation of the nuclear factor (NF)-κB signaling pathway in OA chondrocytes (8), which is

implicated in inflammatory response and cell apoptosis (9). Therefore, the inhibition of both inflammatory cytokines and NF-κB molecules may be considered as a therapeutic target for attenuating the progression of OA.

Artesunate (ART), a semi-synthetic derivative of artemisinin derived from *Artemisia annua*, is one of the most effective clinical treatments for malaria in China (10). This drug has received widespread attention due to its pharmacological properties beyond being an anti-malarial drug. ART was demonstrated to inhibit the expression of TNF-α-induced pro-inflammatory cytokines by repressing the NF-κB pathway in fibroblast-like synoviocytes (11). In addition, ART was effective in suppressing multiple pathogenic factors and inflammation through inhibiting the LPS/TLR4/NF-κB pathway to alleviate hepatic fibrosis (12). Of note, ART was able to decrease the levels of nitric oxide, maintain oxidative homeostasis and inhibit cyclooxygenase (COX)-2 expression and cell apoptosis in rats with rheumatoid arthritis (RA) (13). A recent study also demonstrated that ART attenuated the progression of experimental OA by suppressing the expression of osteoclast-specific and angiogenesis-related genes in the serum and synovium (14). However, the effect of ART on OA chondrocytes remains elusive.

The aim of the present study was to investigate the anti-inflammatory and anti-apoptotic effects and the molecular mechanisms underlying the effects of ART on IL-1β-induced chondrocyte-like ATDC5 cells, as well as the role of ART in a mouse model of OA.

Materials and methods

Materials. ART was purchased from WanXiangHengYuan Technology Co., Ltd. ATDC5 cells were purchased from Riken Cell Bank. Fetal bovine serum (FBS), Dulbecco's modified Eagle's minimum essential medium/Ham's F12 medium (DMEM/F12), penicillin/streptomycin, trypsin and insulin-transferrin-selenite (ITS) were purchased from Invitrogen; Thermo Fisher Scientific, Inc. Alcian Blue 8GX was purchased from Sigma-Aldrich; Merck KGaA. The Cell Counting Kit-8 (CCK-8) was purchased from Dojindo Molecular Technologies, Inc. The primary antibodies against Bax, Bcl-2, cleaved caspase-3, cleaved caspase-7, IκBα, p-IκBα, p65, p-p65, lamin B and β-tubulin were obtained from Cell Signaling Technology, Inc.; MMP-3, MMP-13, ADAMTS-5, COX-2 and β-actin were purchased from Abcam. Three-month-old male C57BL/6 mouse (n=60) were purchased from Vital River.

Cell differentiation and culture. ATDC5 is a murine teratocarcinoma cell line. The cells were cultured in DMEM/F12 with 5% FBS and 1% penicillin/streptomycin in a humidified incubator with 5% CO_2 at 37˚C. Once the cells were 70-80% confluent, the medium was supplemented with 1% ITS. The differentiation medium was changed every 2 days to induce differentiation of the cells into chondrocyte-like cells. To evaluate the level of glycosaminoglycan production, 1% Alcian blue staining was performed, and the mRNA expression levels of collagen (COL) II and COL X were analyzed to further confirm the differentiation level of the ATDC5 cells. The primers used to amplify COL II and COL X in mice are listed in Table I. Finally, ATDC5 cells were used for the experiments after 2 weeks of differentiation in culture.

Table I. Sequences of primers used in quantitative polymerase chain reaction analysis.

Gene	Primer sequences (5'-3')
COL II	
Forward	ACGAAGCGGCTGGCAACCTCA
Reverse	CCCTCGGCCCTCATCTCTACATCA
COL X	
Forward	TGCCCGTGTCTGCTTTTACTGTCA
Reverse	TCAAATGGGATGGGGGCACCTACT
MMP-3	
Forward	ACATGGAGACTTTGTCCCTTTTG
Reverse	TTGGCTGAGTGGTAGAGTCCC
MMP-13	
Forward	TGTTTGCAGAGCACTACTTGAA
Reverse	CAGTCACCTCTAAGCCAAAGAAA
ADAMTS-5	
Forward	GGAGCGAGGCCATTTACAAC
Reverse	CGTAGACAAGGTAGCCCACTTT
COX-2	
Forward	TTCCAATCCATGTCAAAACCGT
Reverse	AGTCCGGG TACAGTCACACTT
β-actin	
Forward	GGCTGTATTCCCCTCCATCG
Reverse	CCAGTTGGTAACAATGCCATGT

COL, collagen; COX, cyclooxygenase; MMP, matrix metalloproteinase; ADAMTS, a disintegrin and metalloproteinase with thrombospondin motifs.

Cell viability. Cell viability was determined using the CCK-8 assay, according to the manufacturer's instructions. The chondrocyte-like ATDC5 cells were divided into two groups: In group 1, the cells were seeded in 96-well plates at a density of 4,000 cells/well and cultured with or without ART (3.125, 6.25, 12.5, 25 and 50 μM) for 24 h; in group 2, the cells were pretreated with ART (3.125, 6.25, 12.5, 25 and 50 μM) for 24 h, then co-incubated with IL-1β (10 ng/ml) for a further 24 h. Subsequently, 10 μl of CCK-8 solution was added to each well and incubated at 37˚C for 2 h. The absorbance at 450 nm was measured using a Multiskan GO microplate reader (Thermo Fisher Scientific, Inc.).

Flow cytometric analysis of cell apoptosis. Cell apoptosis was monitored using a flow cytometry apoptosis detection kit [phycoerythrin (PE)-Annexin V/7-aminoactinomycin (7-ADD) double-fluorescence labelling]. After re-suspending the cells in Annexin V binding buffer, the harvested chondrocyte-like ATDC5 cells ($1x10^5$) were stained with 5 μl PE-Annexin V and 5 μl 7-ADD for 15 min at room temperature in the dark. The stained cells were analyzed with a FACSAria™ II flow cytometer (BD Biosciences) within 1 h.

Table II. Changes in cartilage thickness in different groups and at different time-points.

	HC (mm)			CC (mm)		
Time (days)	Sham	Vehicle	ART	Sham	Vehicle	ART
30	0.79±0.032	0.74±0.041	0.78±0.040	0.34±0.038	0.36±0.041	0.35±0.038
60	0.76±0.092	0.44±0.143[a]	0.75±0.103[b]	0.33±0.110	0.68±0.127[a]	0.36±0.100[b]

The level of significance was set at P<0.05 and indicated by 'a' for the comparison between the vehicle-treated and sham groups, or 'b' for the comparison between the ART-treated and vehicle-treated groups. Values are presented as mean ± standard deviation. CC, calcified cartilage; HC, hyaline cartilage (data on the thickness of CC and HC were obtained from histological sections examined at a magnification of x10).

Reverse transcription-quantitative polymerase chain reaction (RT-qPCR) analysis. Chondrocyte-like ATDC5 cells were washed with cold PBS and incubated with TRIzol reagent (Invitrogen; Thermo Fisher Scientific, Inc.) to extract total RNA. The total RNA was quantified with a spectrophotometer at 260 nm (Thermo Scientific NanoDrop 2000), and the ratio of the absorbance at A260/A280 was used to evaluate the purity of the RNA. cDNA was synthesized using 2 μg RNA with a PrimeScript™ RT Master Mix (Takara Bio, Inc.). cDNA was then subjected to RT-qPCR analysis with SYBR® Fast qPCR Mix (Takara Bio, Inc.) using the CFX96 Real-Time PCR system (Bio-Rad Laboratories, Inc.) under conditions of 94˚C for 30 sec, followed by 40 cycles at 95˚C for 5 sec and 60˚C for 10 sec, and finally the dissociation curve of each primer pair was analyzed to determine primer specificity. The reaction was performed in a total volume of 20 μl (2 μl diluted cDNA, 10 μl SYBR Green Master Mix, 1 μl forward primer, 1 μl reverse primer and 6 μl RNase-free water). Target mRNA levels were normalized to the β-actin level, which was used as a control. Data were analyzed using the $2^{-\Delta\Delta Cq}$ method (15). All the PCRs were performed in triplicate for each gene. The primers used to amplify MMP-3, MMP-13, ADAMTS-5, COX-2 and β-actin in mice are shown in Table II.

Isolation of cytosol and nucleus fractions. To determine the redistribution of p65, a nuclear and cytoplasmic extraction kit (Thermo Fisher Scientific, Inc.) was used. Following ART treatment, the cells were collected, washed twice with cold PBS and then air-dried. Next, the cells were incubated with Cytoplasmic Extraction Reagent (CER)I on ice for 10 min prior to the addition of CER II. After incubation together for 1 min, the cells were centrifuged at 16,000 x g and 4˚C for 5 min, and then the supernatant (cytoplasm extract) was collected. The insoluble fraction was re-suspended in cold NER for 40 min, centrifuged at 16,000 x g and 4˚C for 10 min, and the supernatant (nuclear extract) was then collected. The supernatants were frozen in liquid nitrogen and stored at -80˚C until analysis.

Western blot analysis. The collected chondrocyte-like ATDC5 cells were washed three times with cold PBS, re-suspended in RIPA buffer and incubated on ice for 30 min. The protein concentration was determined using the bicinchoninic acid assay (Bio-Rad Laboratories, Inc.). Equal amounts of protein were subjected to 10% SDS-PAGE and subsequently transferred to PVDF membranes. The membranes were blocked with 5% non-fat milk for 1 h at room temperature and incubated at 4˚C overnight with the primary antibodies against MMP-3 (1:2,000, cat. no. ab52915), MMP-13 (1:3,000, cat. no. ab39012), ADAMTS-5 (1:1,000, cat. no. ab182795), COX-2 (1:1,000, cat. no. ab62331), β-actin (1:2500, cat. no. ab8226) (all from Abcam); Bcl-2 (1:1,000, cat. no. 3498), Bax (1:1,000, cat. no. 14796), cleaved caspase-3 (1:1,000, cat. no. 9654), cleaved caspase-7 (1:1,000, cat. no. 8438), IκBα (1:1,000, cat. no. 4814), p-IκBα (1:1,000, cat. no. 2859), p65 (1:1,000, cat. no. 6956), p-p65 (1:1,000, cat. no. 3036) lamin B (1:5,000, cat. no. 12255), and β-tubulin (1:1,000, cat. no. 2146) (all from Cell Signaling Technology, Inc.). After washing three times with TBST for 5 min, the membranes were incubated with secondary antibodies [peroxidase-conjugated AffiniPure goat anti-rabbit IgG (H + L), 1:800, cat. no. ZB-2301, OriGene Technologies, Inc.] for 2 h. Finally, the immunoreactive bands were detected with the AP chromogenic substrate (Thermo Fisher Scientific, Inc.).

Animal experiments. All experimental procedures were approved by the Institutional Animal Care and Use Committee of First Affiliated Hospital of Xinjiang Medical University (protocol no. IACUC20171129-01). The mice were housed under controlled conditions (temperature, 25±2˚C; light/dark cycle, 12/12 h; relative humidity, 70%). Prior to the anterior cruciate ligament transection (ACLT) surgery, the mice were anesthetized with intravenous injection of 1% pentobarbitone (40 mg/kg). Following a parapatellar incision, the ACL of the right knee was transected to establish the OA model. Then, the joint capsule and skin were sutured layer-by-layer. For the sham group, a parapatellar incision was performed in the right knee joint to expose the ACL, after which time the joint capsule and skin were sutured separately. To identify the optimal dose (100 mg/kg), a preliminary experiment was first performed by using multiple concentrations of ART (50, 100 and 200 mg/kg) injected for 8 weeks postoperatively (Fig. S1). At 50 mg/kg, ART exerted minimal chondroprotective effects, and 200 mg/kg ART induced proteoglycan loss in articular cartilage. Therefore, in the formal experiment, all mice were randomly assigned into the sham, vehicle-treated ACLT and ART (100 mg/kg)-treated ACLT groups (n=20 per group). Either ART (100 mg/kg) or an equivalent volume of 5% $NaHCO_3$ was administered intraperitoneally for 4 and 8 weeks starting on the second postoperative day. A total of 10 mice

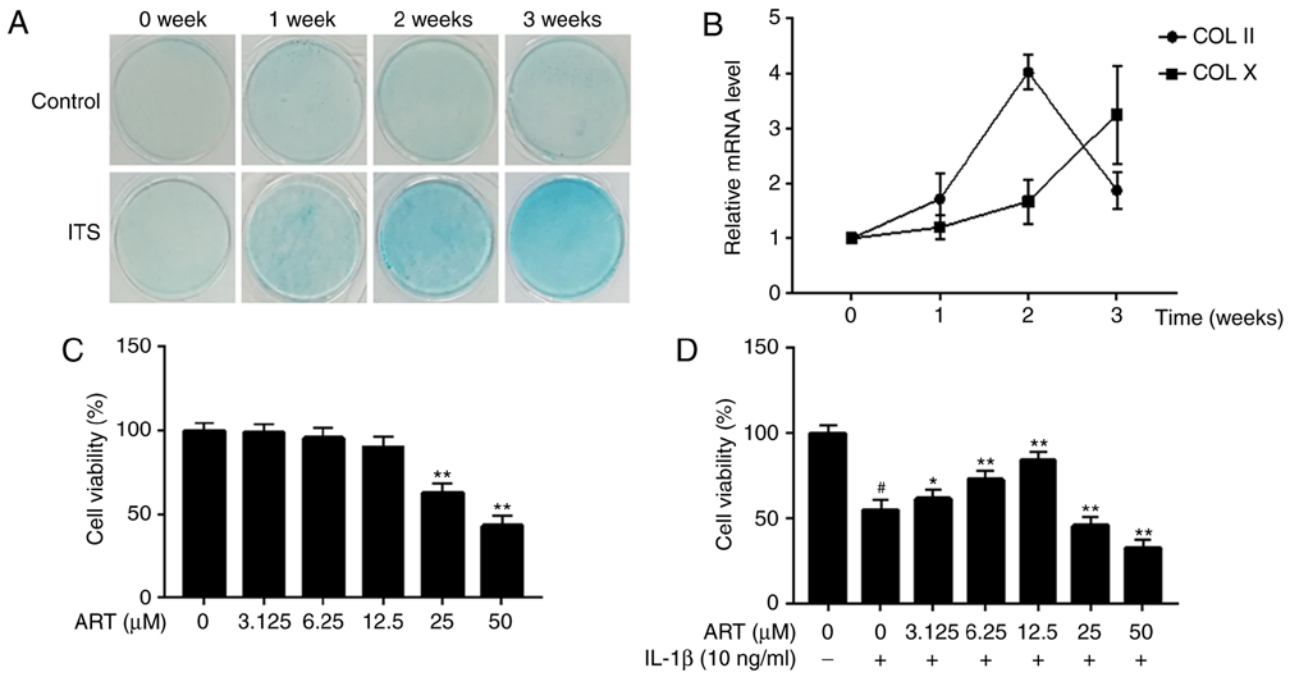

Figure 1. Effects of ART on the viability of chondrocyte-like ATDC5 cells. (A) The differentiation of ATDC5 cells was determined by 1% Alcian blue staining at 0, 1, 2 and 3 weeks. (B) The relative expression of COL II and COL X mRNA was determined by reverse transcription-quantitative polymerase chain reaction analysis. (C) The cells were treated with various concentrations of ART for 24 h, and cell viability was evaluated by the CCK-8 assay. (D) The cells were pretreated for 24 h with various concentrations of ART and then stimulated with IL-1β (10 ng/ml) for 24 h. The cell viability was measured by the CCK-8 assay. The results represent the mean ± standard deviation of three independent experiments. *P<0.05 and **P<0.01 vs. IL-1β-induced group; $^{\#}$P<0.01 vs. control group. ART, artesunate; COL, collagen; IL, interleukin.

from each group were sacrificed at 4 and 8 weeks after experiment completion.

Histological analysis. The right knee joints were dissected and fixed in 10% buffered formalin for 24 h and then decalcified in 10% EDTA (pH 7.3) for 3 weeks. The specimens were embedded in paraffin and cut into 4-μm sections for hematoxylin and eosin (H&E) and safranin O staining. The thickness of the hyaline cartilage (HC) and the calcified cartilage (CC) were measured by H&E staining (thickness of HC, distance from the articular cartilage surface to the tidemark; thickness of CC, distance from the tidemark to the subchondral bone plate). Osteoarthritis Research Society International-modified Mankin criteria (OARSI) scores were calculated for evaluating the state of articular cartilage in each group. All counting was conducted blindly by an author who had not been involved in the experiments.

Statistical analysis. Data are expressed as the means ± standard deviation of the representative experiment performed in triplicate. One-way analysis of variance followed by the Least Significant Difference post hoc test was used to determine whether the differences among groups were statistically significant. SPSS 22.0 (IBM Corp.) was used for all data analyses. P<0.05 was considered to indicate statistically significant differences.

Results

Differentiation of ATDC5 cells. To determine whether ITS induces ATDC5 cells to form cartilage nodules, the cells were treated with ITS for 3 weeks, and 1% Alcian blue staining was performed at 0, 1, 2 and 3 weeks. As shown in Fig. 1A, ITS treatment resulted in a gradual increase in the staining intensity in the ATDC5 cells in a time-dependent manner. Next, the expression of chondrogenic differentiation markers (COL II and COL X) was assessed using RT-qPCR. The data revealed that the mRNA level of COL II increased significantly after 1 week of induction of the chondrocytes, reaching a peak at 2 weeks, suggesting early-stage differentiation of the chondrocytes. The mRNA level of COL X also increased between 0 and 2 weeks, but exceeded the expression level of COL II at 3 weeks, indicating late-stage differentiation of the chondrocytes (Fig. 1B). These results demonstrated that the ATDC5 cells differentiated from proliferative to hypertrophic chondrocytes. Therefore, ATDC5 cells that had been induced for 2 weeks were selected for the following *in vitro* experiments.

Effects of ART on chondrocyte-like ATDC5 cell viability. A CCK-8 assay was performed to investigate the effect of ART on the viability of chondrocyte-like ATDC5 cells and the cells incubated with IL-1β. The results revealed that 25 and 50 μM ART significantly reduced cell viability, whereas concentrations of ≤12.5 μM ART had no harmful effects on cellular viability after treatment for 24 h (Fig. 1C). Furthermore, compared with the control group, a significant decrease in IL-1β-induced cell viability was reversed by ART at lower concentrations (3.125, 6.25 and 12.5 μM) in a dose-dependent manner. However, higher concentrations of ART (25 and 50 μM) significantly reduced cell viability (Fig. 1D). As a result, 3.125, 6.25 and 12.5 μM ART were selected as the low, medium and high concentrations, respectively.

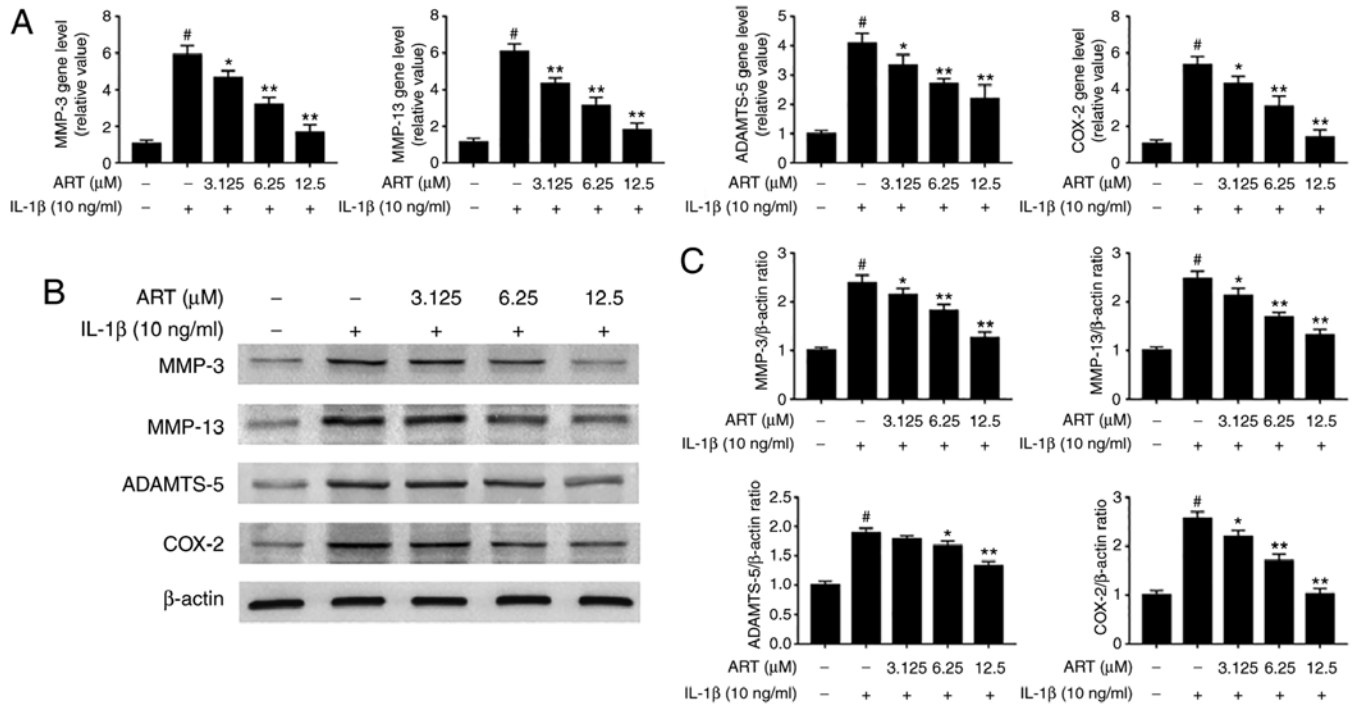

Figure 2. Effects of ART on IL-1β-induced inflammation in chondrocyte-like ATDC5 cells. The cells were pretreated for 24 h with various concentrations of ART and then stimulated with IL-1β (10 ng/ml) for 24 h. Then, mRNA and protein samples were collected. (A-C) The mRNA and protein expression of MMP-3, MMP-13, ADAMTS-5 and COX-2 were detected by reverse transcription-quantitative polymerase chain reaction and western blotting, respectively. The results represent the mean ± standard deviation of three independent experiments. *P<0.05 and **P<0.01 vs. IL-1β-induced group; $^{\#}$P<0.01 vs. control group. ART, artesunate; IL, interleukin; MMP, matrix metalloproteinase; ADAMTS, a disintegrin and metalloproteinase with thrombospondin motifs; COX, cyclooxygenase.

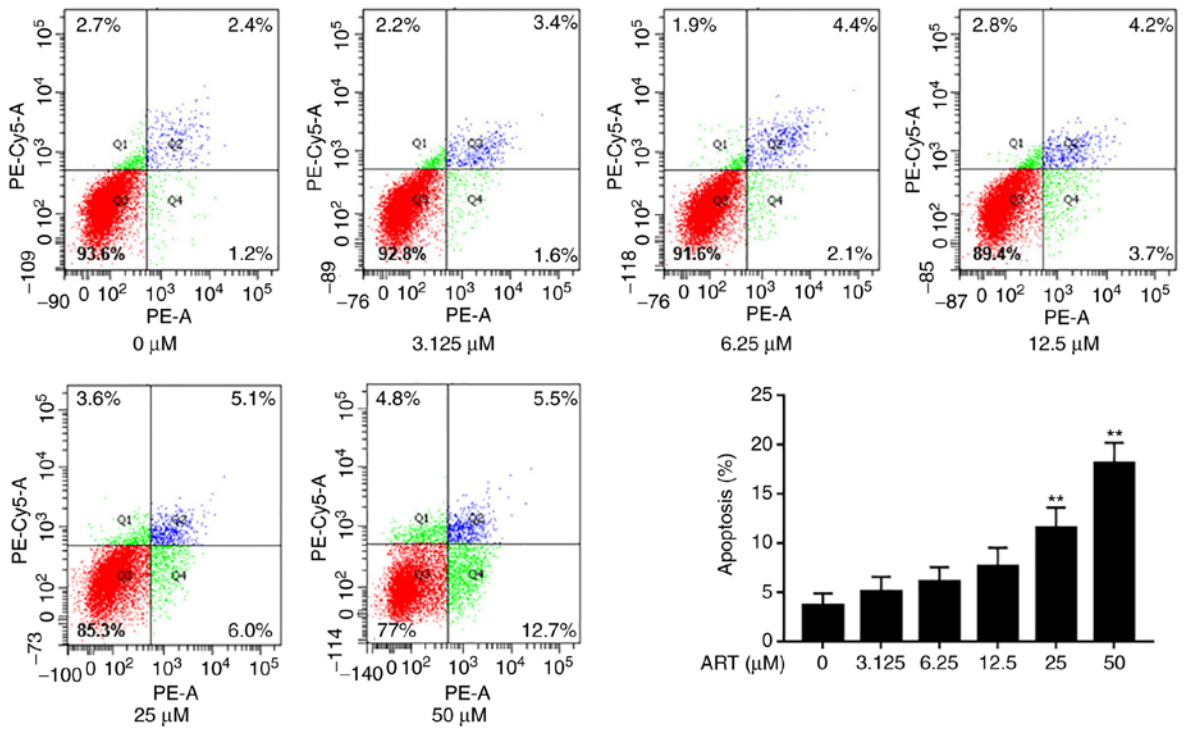

Figure 3. Evaluation of cytotoxicity induced by ART. The chondrocyte-like ATDC5 cells were treated with ART alone for 24 h. The apoptotic rate was determined by flow cytometry using PE-Annexin V/7-ADD double-fluorescence labelling. The apoptotic rate for each group is presented as the mean ± standard deviation of three replicates. **P<0.01 vs. control group. ART, artesunate; PE, phycoerythrin; 7-ADD, 7-amino-actinomycin.

ART reduces the production of inflammatory cytokines in IL-1β-induced chondrocyte-like ATDC5 cells. The anti-inflammatory effect of ART on chondrocyte-like ATDC5 cells induced by IL-1β was next analyzed. The

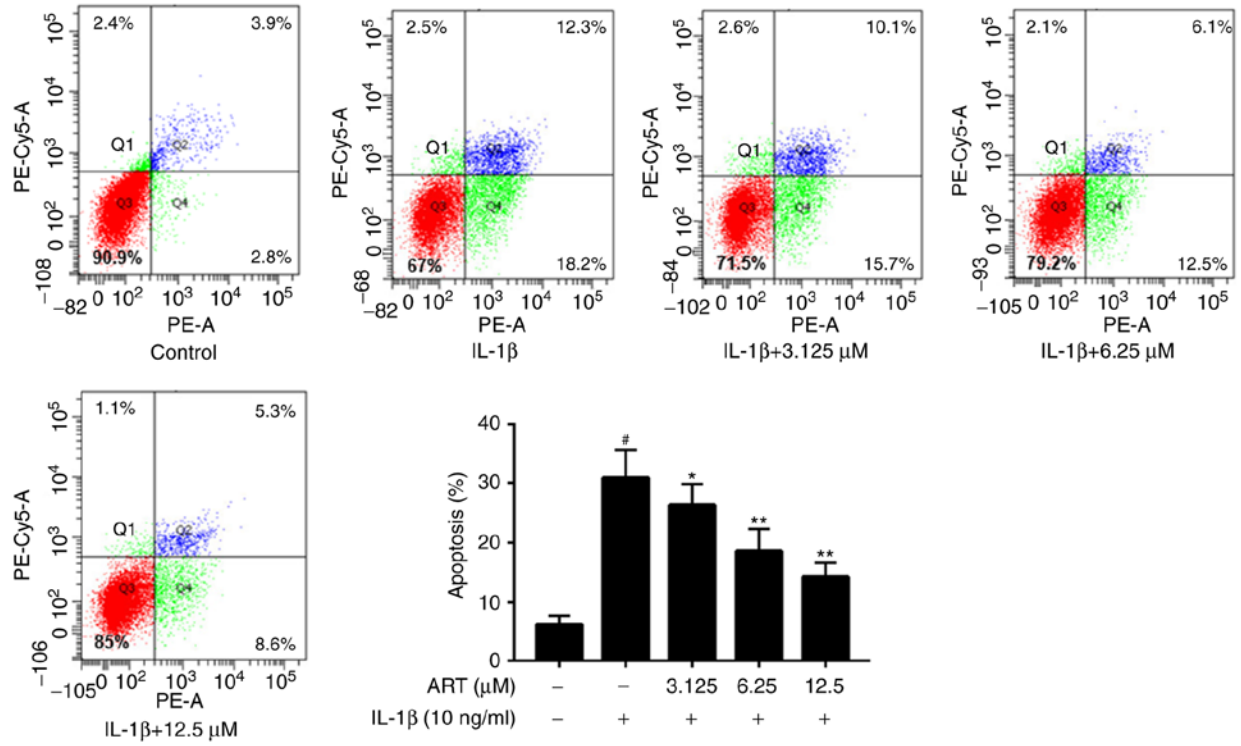

Figure 4. Protective effect of ART against apoptosis in IL-1β-induced chondrocyte-like ATDC5 cells. The cells were pretreated for 24 h with various concentrations of ART and then stimulated with IL-1β (10 ng/ml) for 24 h. The apoptotic rate was determined by flow cytometry using PE-Annexin V/7-ADD double-fluorescence labelling. The apoptotic rate for each group is presented as the mean ± standard deviation of three replicates. *P<0.05 and **P<0.01 vs. IL-1β-induced group; $^{\#}$P<0.01 vs. control group. ART, artesunate; IL, interleukin; PE, phycoerythrin; 7-ADD, 7-amino-actinomycin.

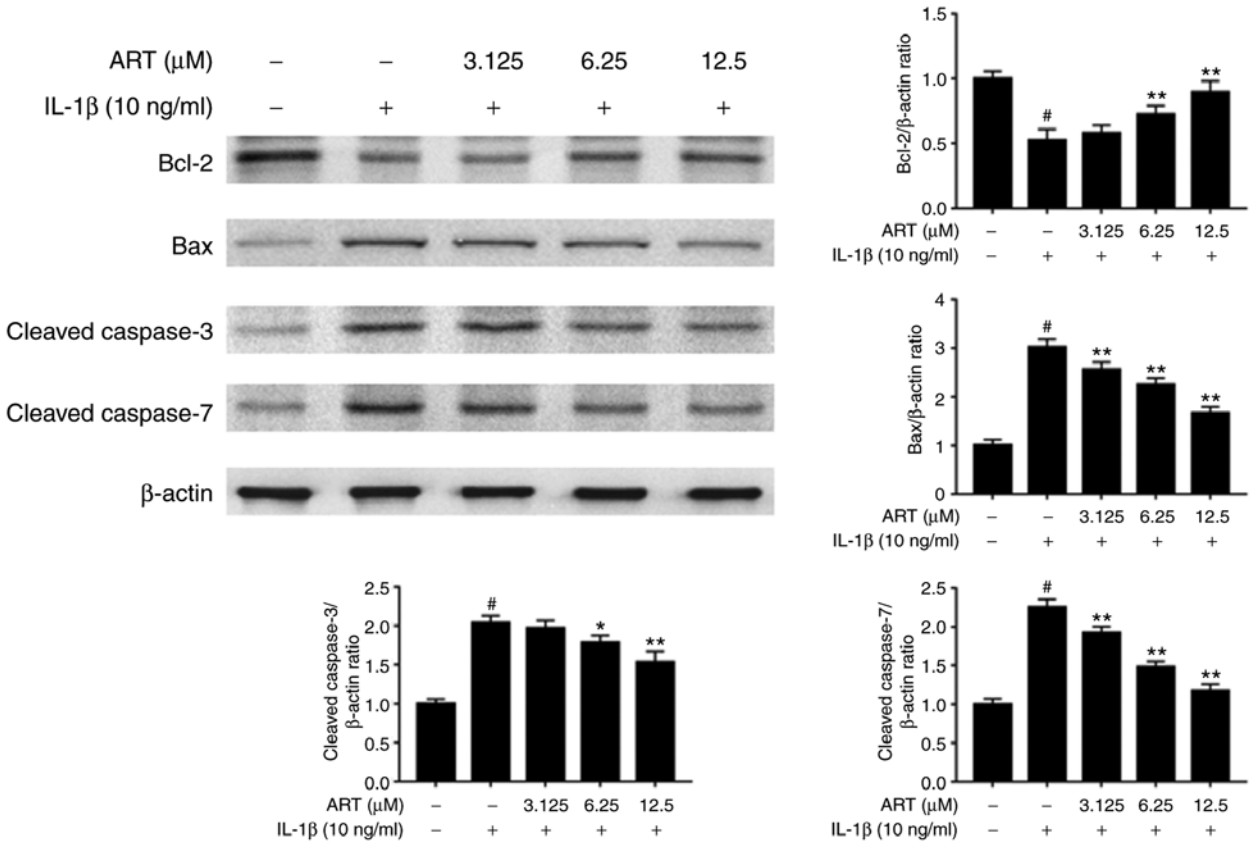

Figure 5. Suppression of apoptosis by ART in IL-1β-induced chondrocyte-like ATDC5 cells. The cells were pretreated for 24 h with various concentrations of ART and then stimulated with IL-1β (10 ng/ml) for 24 h. Western blotting and quantification analysis were performed to analyze the protein expression of Bcl-2, Bax, cleaved caspase-3 and cleaved caspase-7. The results represent the mean ± standard deviation of three independent experiments. *P<0.05 and **P<0.01 vs. IL-1β-induced group; $^{\#}$P<0.01 vs. control group. ART, artesunate; IL, interleukin.

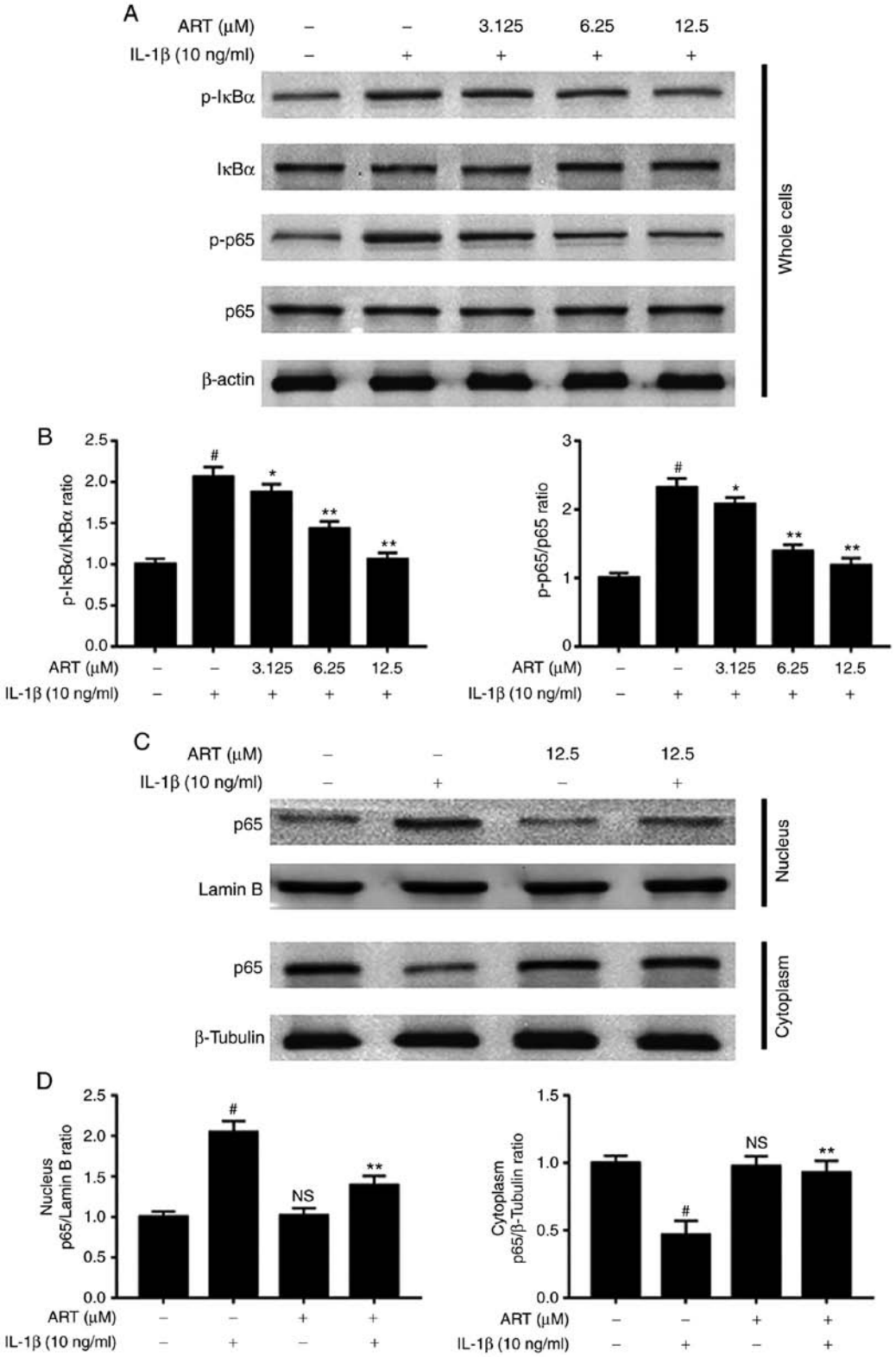

Figure 6. Inhibition of NF-κB activity by ART in chondrocyte-like ATDC5 cells stimulated by IL-1β. The cells were pretreated for 24 h with ART and then stimulated with IL-1β (10 ng/ml) for 24 h. (A and B) The protein levels of p-IκBα, IκBα, p-p65 and p65 were detected by western blotting and the ratios of p-IκBα/IκBα and p-p65/p65 were assessed by quantification analysis. (C and D) The presence of p65 in the cytosolic and nuclear extracts was determined by western blotting. β-Tubulin and lamin B served as the loading controls for the cytosolic and nuclear fractions, respectively. Data are presented as the mean ± standard deviation of three independent experiments. *P<0.05 and **P<0.01 vs. IL-1β-induced group; $^{\#}$P<0.01 vs. control group; NS (not significant) vs. control group. ART, artesunate; IL, interleukin; NF, nuclear factor.

mRNA and protein expression levels of inflammatory factors were evaluated by RT-qPCR and western blot analysis, respectively. The results revealed that MMP-3, MMP-13, ADAMTS-5 and COX-2 were prominently upregulated in the chondrocyte-like ATDC5 cells exposed to 10 ng/ml IL-1β for 24 h. Both the gene and protein levels

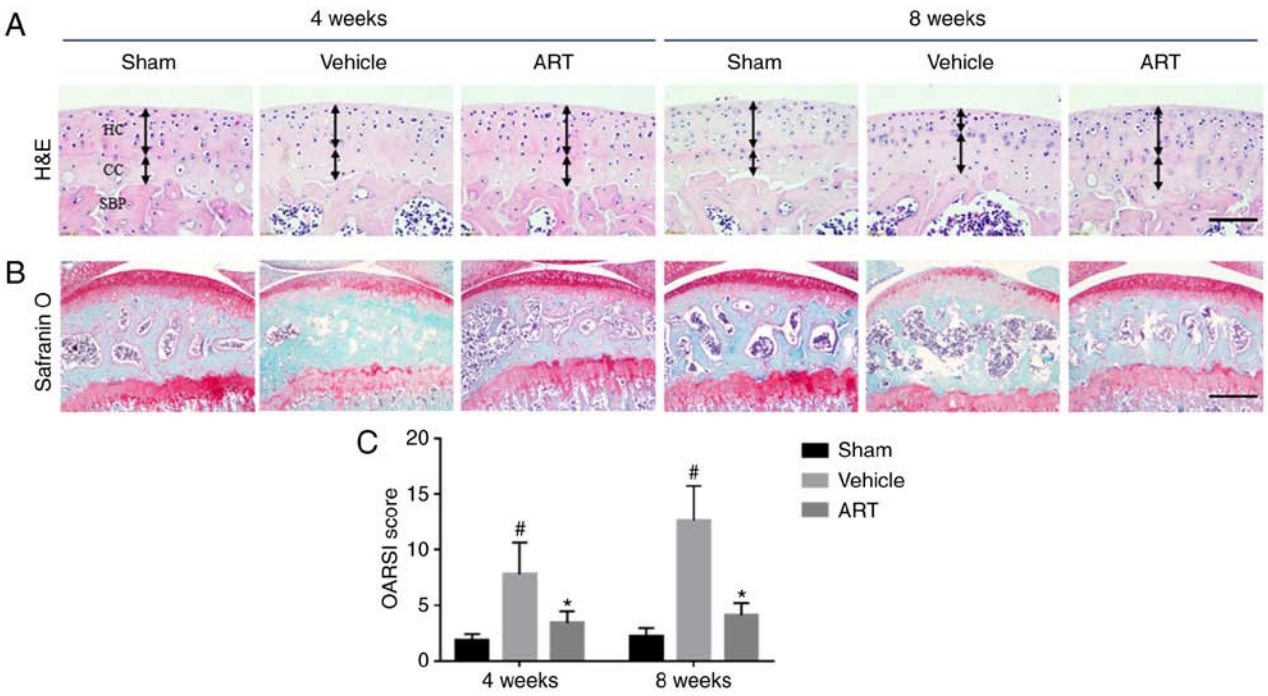

Figure 7. Chondroprotective effects of ART on an ACLT mouse model at postoperative weeks 4 and 8 in the formal experiment. (A and B) Histological analysis of articular cartilage was performed following H&E staining (scale bar: 100 μm) and Safranin O staining (scale bar, 400 μm), n=10/group. (A) Changes in the thickness of HC and CC following sham surgery or ACLT surgery. (B) Safranin O staining of sagittal sections of the tibial medial compartment were performed, where proteoglycan appears as red and bone as blue. (C) OARSI scores of articular cartilage were calculated for each group. The data in the figures represent the mean ± standard deviation. Significant differences among groups are indicated as *P<0.05 vs. vehicle group and $^{\#}$P<0.05 vs. sham group. Representative histological images are shown. ART, artesunate; ACLT, anterior cruciate ligament transection; H&E, hematoxylin and eosin; HC, hyaline cartilage; CC, calcified cartilage; OARSI, Osteoarthritis Research Society International-modified Mankin criteria.

of MMP-3, MMP-13 and COX-2 were reduced by ART treatment in a dose-dependent manner. Although 3.125 μM ART failed to inhibit the protein expression of ADAMTS-5, ART at concentrations of 6.25 μM and 12.5 μM reduced the expression of ADAMTS-5 at the gene and protein levels (Fig. 2A-C). Taken together, these results indicated that ART suppressed the inflammatory response by downregulating the expression of inflammatory cytokines at both the gene and protein levels.

ART inhibits IL-1β-induced apoptosis in chondrocyte-like ATDC5 cells. To assess the effect of ART on cell apoptosis induced by IL-1β, flow cytometry and western blot analysis were performed. First, the chondrocyte-like ATDC5 cells were treated with ART at different concentrations for 24 h to assess the drug cytotoxicity. The results demonstrated that ART was only mildly cytotoxic at lower concentrations (3.125, 6.25 and 12.5 μM), but highly cytotoxic at higher concentrations (25 and 50 μM), which was consistent with the results of the CCK-8 assay (Fig. 3). Furthermore, compared with the control group, the percentage of apoptotic cells was found to be markedly increased in the IL-1β-treated group, while this increase was attenuated by ART treatment in a dose-independent manner (Fig. 4).

To further investigate the effect of ART on the mitochondrial apoptosis pathway, the protein levels of the anti-apoptotic factor Bcl-2 and the pro-apoptotic factors Bax, cleaved caspase-3 and cleaved caspase-7 were detected by western blotting. The results demonstrated that IL-1β significantly decreased the expression of Bcl-2 and increased the expression of Bax, cleaved caspase-3 and cleaved caspase-7, while these effects were partially reversed by ART (Fig. 5). Taken together, these results suggested that ART played an anti-apoptotic role in IL-1β-induced chondrocyte-like ATDC5 cells.

ART represses the NF-κB signaling pathway in IL-1β-induced chondrocyte-like ATDC5 cells. To explore the molecular mechanism through which ART exerts anti-inflammatory and anti-apoptotic effects on IL-1β-induced chondrocyte-like ATDC5 cells, western blot analysis was performed to detect changes in the NF-κB signaling pathway. The results demonstrated that the expression levels of p-IκBα and p-p65 were markedly increased in the IL-1β-induced group compared with the control group. Moreover, stimulation of chondrocyte-like ATDC5 cells with IL-1β resulted in marked degradation of IκBα. However, ART significantly repressed the IL-1β-induced phosphorylation of IκBα and p65 and degradation of IκBα (Fig. 6A and B). In addition, as NF-κB activation requires the nuclear translocation of p65, we further investigated the effect of ART on the redistribution of p65 in the cytoplasm and nucleus. The results demonstrated that IL-1β significantly increased the nuclear translocation of p65. By contrast, ART treatment effectively upregulated the cytosolic levels and downregulated the nuclear levels of the p65 protein (Fig. 6C and D). Moreover, the use of ART alone failed to affect the expression of p65 in the cytoplasm and the nucleus (Fig. 6C and D). Taken together, these findings demonstrated that treatment with ART significantly inhibited NF-κB signaling.

ART attenuates the progression of ACLT-induced OA in mice. Finally, ART was administered intraperitoneally to mice after the ACLT procedure to investigate its chondroprotective effects. H&E staining revealed an increase in CC thickness in the vehicle-treated group relative to the sham group at postoperative week 8, which was delayed by ART treatment (Fig. 7A and Table II). Safranin O staining demonstrated that the loss of proteoglycan was significantly attenuated in the ART-treated group compared with the vehicle-treated group at postoperative weeks 4 and 8 (Fig. 7B), which was supported by the OARSI scores (Fig. 7C). These results indicated that ART exerted strong protective effects on articular cartilage in OA.

Discussion

Currently available pharmacological treatments have failed to halt or reverse the progression of OA, and are accompanied by a variety of side effects (16). Thus, bioactive small molecules from natural herbage that may be suitable for OA treatment have recently been drawing attention, particularly those with minimal or no side effects (17-19). ART, a bioactive small molecule, has been used to treat various ailments ranging from malaria to tumors and RA (20). To the best of our knowledge, the present study was the first to demonstrate that ART treatment suppressed the expression of inflammatory mediators at both the gene and protein levels, and inhibited apoptosis in IL-1β-induced chondrocyte-like ATDC5 cells, which was associated with the inactivation of the NF-κB signaling pathway. In addition, ART treatment exerted protective effects on articular cartilage in an ACLT mouse model.

In healthy chondrocytes, the synthesis and degradation of ECM are in dynamic balance. However, this balance is disrupted by reduced anabolic and elevated catabolic capacities of OA chondrocytes (21). Previous studies have indicated that MMPs and ADAMTs are responsible for degrading type II collagen and proteoglycan in ECM, and the suppression of these enzymes has the ability to attenuate articular cartilage degeneration (22,23). According to the findings of the present study, in the presence of IL-β, ART treatment inhibited the catabolism of ECM components by downregulating MMP-3, MMP-13 and ADAMTS-5.

COX-2 is an important inflammatory mediator that contributes to prostaglandin E2 (PGE2) generation (24). Increased PGE2 levels lead to activation of MMPs and other inflammatory cytokines (25), thereby perpetuating a pathogenic circle in the OA cartilage. In the present study, COX-2 was markedly elevated following IL-1β stimulation and was reduced by ART treatment in a dose-dependent manner. Moreover, the downregulation of COX-2 may alleviate the catabolism and inflammatory response, thus delaying the progression of OA. Additionally, ART has been reported to suppress the expression of other catabolic genes, including MMP-2 and MMP-9 (26), and angiogenesis-related cytokines, such as VEGF and HIF-1α (27). Taken together, these findings indicate that ART exerts strong anti-inflammatory protective effects in OA chondrocytes.

The apoptosis of chondrocytes is closely associated with OA development. It is widely accepted that increased IL-1β induces apoptosis of chondrocytes through upregulating pro-apoptotic and downregulating anti-apoptotic proteins, thereby accelerating cartilage degradation (7). In OA chondrocytes, the expression of the pro-apoptotic factors Bax, cleaved caspase-3 and cleaved caspase-7 are higher than normal, while the expression of the anti-apoptotic factor Bcl-2 is lower (28,29). Our findings were in agreement with those of previous reports. Moreover, we found that ART reduced the occurrence of apoptosis in a dose-dependent manner. In addition, ART not only decreased the expression of Bax, cleaved caspase-3 and cleaved caspase-7, but also enhanced the expression of Bcl-2. Taken together, these observations confirm that ART exerts an anti-apoptotic effect on OA chondrocytes. However, several studies have reported that ART induces apoptosis in some tumor cell lines (30,31). It may be hypothesized that these differences are due to the different doses or action times of ART treatment and the different cell types used in the experiments.

The NF-κB family of transcription factors plays a key role in the regulation of inflammation, immune response, and cell proliferation and apoptosis (32). Inappropriate NF-κB activity not only exaggerates the inflammation of chondrocytes via promoting the overexpression of inflammatory genes, but also accelerates the apoptosis of chondrocytes by disrupting the expression of apoptosis-related proteins (33). Therefore, targeted inhibition of the NF-κB pathway may be beneficial for the treatment of OA. The present study demonstrated that ART inhibited the IL-1β-induced phosphorylation of IκBα and p65, as well as the degradation of IκBα. Importantly, ART treatment repressed the translocation of p65 from the cytoplasm to the nucleus and improved the redistribution of p65, supporting that ART had no obvious effect on the total expression of p65 in the cells. Collectively, these findings suggest that inactivation of NF-κB signaling is one of the mechanisms by which ART plays a protective role in OA chondrocytes.

In this study, an unstable and mechanical-loading OA model was established by transecting the ACL in mice. Histological analysis revealed an increase in CC thickness in the vehicle group at postoperative week 8, while this change was not synchronized with the loss of proteoglycan, which began on postoperative week 4. This finding is consistent with a previous study (34) and warrants further investigation by exploring potential cell signaling mechanisms in subchondral bone. Moreover, the histological scoring of OA increased over time in the vehicle-treated group. However, ATR administration not only inhibited the increase in CC thickness and the loss of proteoglycan, but also lowered the histological scoring of OA. These findings indicate that ART delays the progression of OA.

In summary, the present study revealed that ART protected chondrocytes against inflammation and apoptosis *in vitro* and attenuated articular cartilage degeneration *in vivo*, indicating that ART may be a promising potential preventive therapy for OA.

Acknowledgements

Not applicable.

Funding

The present study was supported by grants from the National Natural Science Foundation of China (nos. U1503221 and 81860746).

Availability of data and materials

The datasets generated and analyzed in the present study are available from the corresponding author on reasonable request.

Authors' contributions

All the authors have read and approved the final version of this manuscript. YL, WM and LC designed the research and wrote the paper. YL, WM, JR and SW performed the experiments. TW and BJ analyzed the data and edited the paper. HM and AA contributed the materials and reagents. YL, KZ and LC revised the manuscript and guided the research.

Ethics approval and consent to participate

All experimental procedures were approved by the Institutional Animal Care and Use Committee of First Affiliated Hospital of Xinjiang Medical University (protocol no. IACUC20171129-01).

Patient consent for publication

Not applicable.

Competing interests

The authors declare that they have no competing interests.

References

1. Helmick CG, Felson DT, Lawrence RC, Gabriel S, Hirsch R, Kwoh CK, Liang MH, Kremers HM, Mayes MD, Merkel PA, *et al*: Estimates of the prevalence of arthritis and other rheumatic conditions in the United States. Part I. Arthritis Rheum 58: 15-25, 2008.
2. Chen D, Shen J, Zhao W, Wang T, Han L, Hamilton JL and Im HJ: Osteoarthritis: Toward a comprehensive understanding of pathological mechanism. Bone Res 5: 16044, 2017.
3. Cross M, Smith E, Hoy D, Nolte S, Ackerman I, Fransen M, Bridgett L, Williams S, Guillemin F, Hill CL, *et al*: The global burden of hip and knee osteoarthritis: Estimates from the global burden of disease 2010 study. Ann Rheum Dis 73: 1323-1330, 2014.
4. Poole AR, Kobayashi M, Yasuda T, Laverty S, Mwale F, Kojima T, Sakai T, Wahl C, El-Maadawy S, Webb G, *et al*: Type II collagen degradation and its regulation in articular cartilage in osteoarthritis. Ann Rheum Dis 61 (Suppl 2): ii78-ii81, 2002.
5. Kobayashi M, Squires GR, Mousa A, Tanzer M, Zukor DJ, Antoniou J, Feige U and Poole AR: Role of interleukin-1 and tumor necrosis factor alpha in matrix degradation of human osteoarthritic cartilage. Arthritis Rheum 52: 128-135, 2005.
6. Wang M, Shen J, Jin H, Im HJ, Sandy J and Chen D: Recent progress in understanding molecular mechanisms of cartilage degeneration during osteoarthritis. Ann N Y Acad Sci 1240: 61-69, 2011.
7. Wang F, Wu L, Li L and Chen S: Monotropein exerts protective effects against IL-1β-induced apoptosis and catabolic responses on osteoarthritis chondrocytes. Int Immunopharmacol 23: 575-580, 2014.
8. Rigoglou S and Papavassiliou AG: The NF-κB signalling pathway in osteoarthritis. Int J Biochem Cell Biol 45: 2580-2584, 2013.
9. Pan T, Chen R, Wu D, Cai N, Shi X, Li B and Pan J: Alpha-Mangostin suppresses interleukin-1β-induced apoptosis in rat chondrocytes by inhibiting the NF-κB signaling pathway and delays the progression of osteoarthritis in a rat model. Int Immunopharmacol 52: 156-162, 2017.
10. Du Y, Chen G, Zhang X, Yu C, Cao Y and Cui L: Artesunate and erythropoietin synergistically improve the outcome of experimental cerebral malaria. Int Immunopharmacol 48: 219-230, 2017.
11. Xu H, He Y, Yang X, Liang L, Zhan Z, Ye Y, Yang X, Lian F and Sun L: Anti-malarial agent artesunate inhibits TNF-alpha-induced production of proinflammatory cytokines via inhibition of NF-kappaB and PI3 kinase/Akt signal pathway in human rheumatoid arthritis fibroblast-like synoviocytes. Rheumatology (Oxford) 46: 920-926, 2007.
12. Lai L, Chen Y, Tian X, Li X, Zhang X, Lei J, Bi Y, Fang B and Song X: Artesunate alleviates hepatic fibrosis induced by multiple pathogenic factors and inflammation through the inhibition of LPS/TLR4/NF-κB signaling pathway in rats. Eur J Pharmacol 765: 234-241, 2015.
13. Guruprasad B, Chaudhary P, Choedon T and Kumar VL: Artesunate ameliorates functional limitations in Freund's complete adjuvant-induced monoarthritis in rat by maintaining oxidative homeostasis and inhibiting COX-2 expression. Inflammation 38: 1028-1035, 2015.
14. Zhao C, Liu Q and Wang K: Artesunate attenuates ACLT-induced osteoarthritis by suppressing osteoclastogenesis and aberrant angiogenesis. Biomed Pharmacother 96: 410-416, 2017.
15. Livak KJ and Schmittgen TD: Analysis of relative gene expression data using real-time quantitative PCR and the 2(-Delta Delta C(T)) method. Methods 25: 402-408, 2001.
16. Le Graverand-Gastineau MP: Disease modifying osteoarthritis drugs: Facing development challenges and choosing molecular targets. Curr Drug Targets 11: 528-535, 2010.
17. Lu C, Li Y, Hu S, Cai Y, Yang Z and Peng K: Scoparone prevents IL-1β-induced inflammatory response in human osteoarthritis chondrocytes through the PI3K/Akt/NF-κB pathway. Biomed Pharmacother 106: 1169-1174, 2018.
18. Liu M, Zhong S, Kong R, Shao H, Wang C, Piao H, Lv W, Chu X and Zhao Y: Paeonol alleviates interleukin-1β-induced inflammatory responses in chondrocytes during osteoarthritis. Biomed Pharmacother 95: 914-921, 2017.
19. Feng Z, Zheng W, Li X, Lin J, Xie C, Li H, Cheng L, Wu A and Ni W: Cryptotanshinone protects against IL-1β-induced inflammation in human osteoarthritis chondrocytes and ameliorates the progression of osteoarthritis in mice. Int Immunopharmacol 50: 161-167, 2017.
20. Ho WE, Peh HY, Chan TK and Wong WS: Artemisinins: Pharmacological actions beyond anti-malarial. Pharmacol Ther 142: 126-139, 2014.
21. Pereira D, Ramos E and Branco J: Osteoarthritis. Acta Med Port 28: 99-106, 2015.
22. Tetlow LC, Adlam DJ and Woolley DE: Matrix metalloproteinase and proinflammatory cytokine production by chondrocytes of human osteoarthritic cartilage: Associations with degenerative changes. Arthritis Rheum 44: 585-594, 2001.
23. Verma P and Dalal K: ADAMTS-4 and ADAMTS-5: Key enzymes in osteoarthritis. J Cell Biochem 112: 3507-3514, 2011.
24. Nakao S, Ogtata Y, Shimizu E, Yamazaki M, Furuyama S and Sugiya H: Tumor necrosis factor alpha (TNF-alpha)-induced prostaglandin E2 release is mediated by the activation of cyclooxygenase-2 (COX-2) transcription via NFkappaB in human gingival fibroblasts. Mol Cell Biochem 238: 11-18, 2002.
25. Liu B, Goode AP, Carter TE, Utturkar GM, Huebner JL, Taylor DC, Moorman CT III, Garrett WE, Kraus VB, Guilak F, *et al*: Matrix metalloproteinase activity and prostaglandin E2 are elevated in the synovial fluid of meniscus tear patients. Connect Tissue Res 58: 305-316, 2017.
26. Li Y, Wang S, Wang Y, Zhou C, Chen G, Shen W, Li C, Lin W, Lin S, Huang H, *et al*: Inhibitory effect of the antimalarial agent artesunate on collagen-induced arthritis in rats through nuclear factor kappa B and mitogen-activated protein kinase signaling pathway. Transl Res 161: 89-98, 2013.
27. He Y, Fan J, Lin H, Yang X, Ye Y, Liang L, Zhan Z, Dong X, Sun L and Xu H: The anti-malaria agent artesunate inhibits expression of vascular endothelial growth factor and hypoxia-inducible factor-1α in human rheumatoid arthritis fibroblast-like synoviocyte. Rheumatol Int 31: 53-60, 2011.
28. Na JY, Kim S, Song K, Lim KH, Shin GW, Kim JH, Kim B, Kwon YB and Kwon J: Anti-apoptotic activity of Ginsenoside Rb1 in hydrogen peroxide-treated chondrocytes: Stabilization of mitochondria and the inhibition of caspase-3. J Ginseng Res 36: 242-247, 2012.

29. Musumeci G, Castrogiovanni P, Mazzone V, Szychlinska MA, Castorina S and Loreto C: Histochemistry as a unique approach for investigating normal and osteoarthritic cartilage. Eur J Histochem 58: 2371, 2014.
30. Qin G, Wu L, Liu H, Pang Y, Zhao C, Wu S, Wang X and Chen T: Artesunate induces apoptosis via a ROS-independent and Bax-mediated intrinsic pathway in HepG2 cells. Exp Cell Res 336: 308-317, 2015.
31. Zhang P, Luo HS, Li M and Tan SY: Artesunate inhibits the growth and induces apoptosis of human gastric cancer cells by downregulating COX-2. Onco Targets Ther 8: 845-854, 2015.
32. Marcu KB, Otero M, Olivotto E, Borzi RM and Goldring MB: NF-kappaB signaling: Multiple angles to target OA. Curr Drug Targets 11: 599-613, 2010.
33. Pan T, Shi X, Chen H, Chen R, Wu D, Lin Z, Zhang J and Pan J: Geniposide suppresses interleukin-1β-induced inflammation and apoptosis in rat chondrocytes via the PI3K/Akt/NF-κB signaling pathway. Inflammation 41: 390-399, 2018.
34. Cui Z, Crane J, Xie H, Jin X, Zhen G, Li C, Xie L, Wang L, Bian Q, Qiu T, *et al*: Halofuginone attenuates osteoarthritis by inhibition of TGF-β activity and H-type vessel formation in subchondral bone. Ann Rheum Dis 75: 1714-1721, 2016.